Wisconsin Geological
and Natural History Survey
DIVISION OF EXTENSION
UNIVERSITY OF WISCONSIN–MADISON

Hydrogeology of the sandy uplands of the Bayfield Peninsula, Wisconsin

Final report to U.S. Forest Service

USFS Agreement No. 15-GN-11091300-1096

December 15, 2022

Anna C. Fehling[a,*], J. Elmo Rawling III[a], Grace E. Graham[a], Peter M. Chase[a], Susan K. Swanson[b]

[a] Wisconsin Geological and Natural History Survey
[b] Beloit College
* current affiliation: Wisconsin Department of Natural Resources

Open-File Report 2022-04 | 2022

This material is based upon work supported by the U.S. Forest Service under Agreement No. 15-GN-11091300-1096. The views and conclusions contained in this document are those of the authors and should not be interpreted as representing the opinions or policies of the U.S. Forest Service. Mention of trade names or commercial products does not constitute their endorsement by the U.S. Forest Service.

Contents

Introduction

The sandy upland region of the Bayfield Peninsula in northern Wisconsin (fig. 1) is a primary groundwater recharge area for Bayfield County, yet its hydrogeology is poorly understood (Fehling and others, 2018; Graham and others, 2019). The region is largely undeveloped with few wells and the water table is several hundred feet deep, making inferences about the subsurface difficult (Graham and others, 2019). Groundwater recharge to this sandy region provides baseflow for Bayfield Peninsula streams (Fitzpatrick and others, 2015) and supplies groundwater for drinking-water wells. Although groundwater in the region is pristine, it is vulnerable to contamination due to rapid flow paths and potentially little contaminant attenuation in the unsaturated sand (Fehling and others, 2018). Due to the presence of a groundwater divide that splits northern Bayfield County along the Bayfield Peninsula, contamination in the sandy uplands could affect groundwater sources throughout the county (Graham and others, 2019).

The U.S. Forest Service (USFS) is engaged in the stewardship of water resources on National Forest lands, and has been collaborating with the Wisconsin Geological and Natural History Survey (WGNHS) on groundwater studies for more than a decade (e.g., Bradbury and others, 2018; Fehling and others, 2018; Fehling and Hart, 2021). A study to collect new hydrogeologic

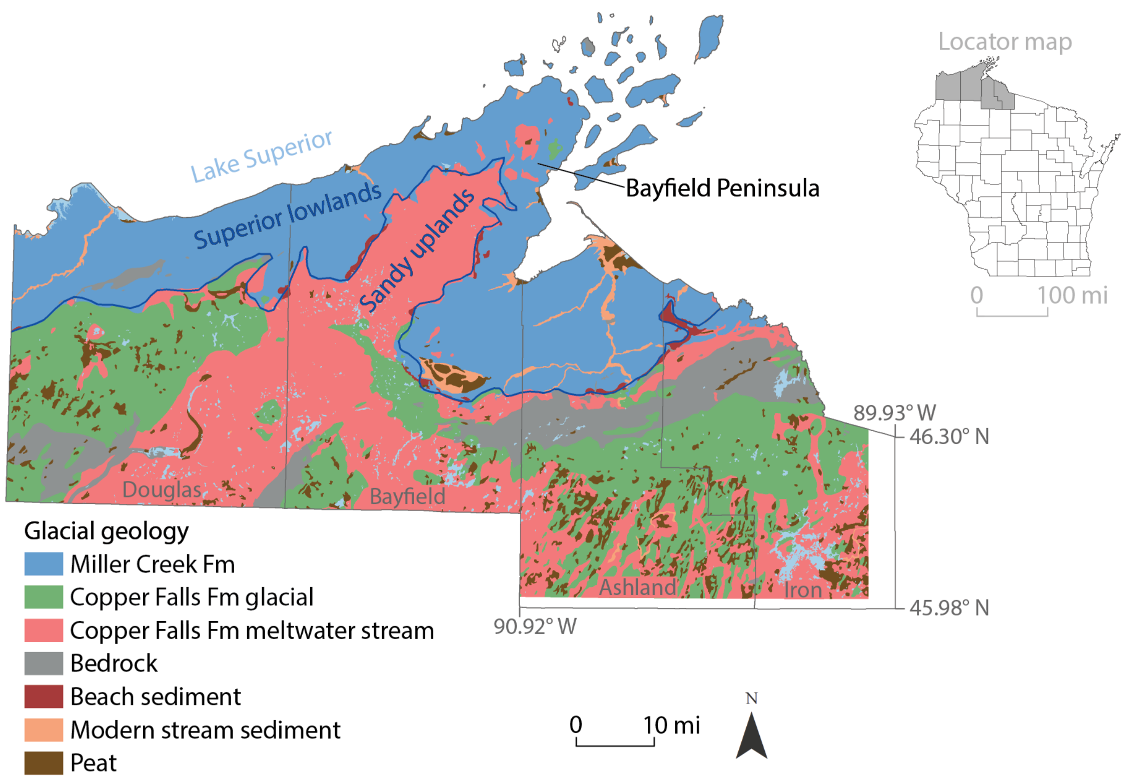

Figure 1: *Map of surficial geology and geologic regions (modified from Clayton, 1984; Graham and others, 2019) in the study area in northern Wisconsin. Counties outlined in gray; names given in gray text. Inset map shows location of studied area in Wisconsin. Fm: formation.*

information from the sandy uplands of the Bayfield Peninsula was funded by the USFS beginning in 2018. A better understanding of the groundwater system will help guide the management of surface water resources such as the Bayfield Peninsula streams, assess potential risks of groundwater contamination from sources such as an oil pipeline that crosses the region (Troy Thompson, USFS, oral commun., 2020), inform wellhead protection in downgradient wells, and contribute to future local and regional hydrogeologic studies.

Purpose and scope

The purpose of this study was to collect new hydrogeological data in the sandy uplands of Bayfield County. To this end, rotosonic cores were drilled and water-table wells installed in July 2020 at two locations in the sandy uplands (fig. 2). An existing well at Horseshoe Lake Campground (Wisconsin Unique Well Number KN002; fig. 2) was outfitted with an air line, which is a nonintrusive method for measuring the water level in a well (Cunningham and Schalk, 2011). Water samples from these three wells and a nearby undeveloped lake (Horseshoe Lake) were analyzed for baseline chemistry. Data were collected between 2019 and 2022. This report describes the geology, water levels, and water chemistry in the sandy uplands.

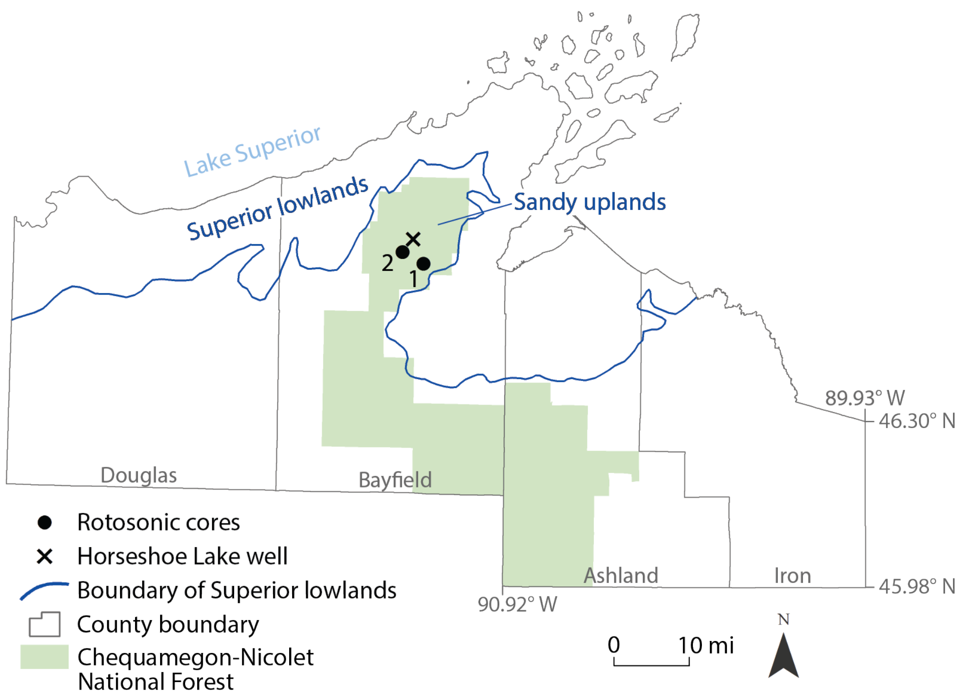

Figure 2. *Map of northern Wisconsin showing location of new rotosonic cores and wells used in this study. Rotosonic cores were co-located with the two new wells. 1: well MW1 with associated rotosonic core RW1; 2: well MW2 with associated rotosonic core RW2 (see tables 1 and 2 for core and well details). County names given in gray.*

Setting

Quaternary geology

Wisconsin's Lake Superior region (fig. 1) was glaciated multiple times in the Quaternary. During the most recent glaciation, the late Wisconsin (ca. 25–11.5 yr B.P.), the Superior Lobe of the Laurentide Ice Sheet covered the region and reached a maximum extent to the south (fig. 3). Ice flowed from the northeast through the Superior Basin until it was thick enough to spill over the regional bedrock divide, forming the Chippewa Lobe (figs. 3 and 4). This ice was subject to stagnation whenever the ice profile in the Superior Basin lowered, and most of the ice margin indicators south of the bedrock divide of the Chippewa Lobe consist of broad (10s of kilometers) zones of stagnant ice features such as disintegration ridges, ice-walled lakes, and kettles. As the ice retreated north of the bedrock divide, the Superior and Chippewa lobes separated, forming an interlobate zone in the vicinity of the study area composed of ice marginal fans (fig. 4).

Sandy till, meltwater stream sediments, and lake sediments of the Copper Falls Formation were deposited when the Superior Lobe was at its maximum and as it retreated into the Superior Basin, before ca. 11,500 yr B.P. (Syverson and others, 2011). Following this retreat into the Superior Basin, the Superior Lobe readvanced partially into the Superior Region between ca. 11,500 yr B.P. and ca. 9,500 yr B.P. This ice surrounded the sandy uplands of the Bayfield Peninsula, formed extensive proglacial lakes in the Superior lowlands, and deposited the clay-rich till of the Miller Creek Formation (Clayton, 1984; Breckenridge, 2013; fig. 1). The resulting landscape has two distinct areas: the low-relief, clay-till plains of the Superior lowlands, and the rolling hills of the sandy uplands (fig. 1).

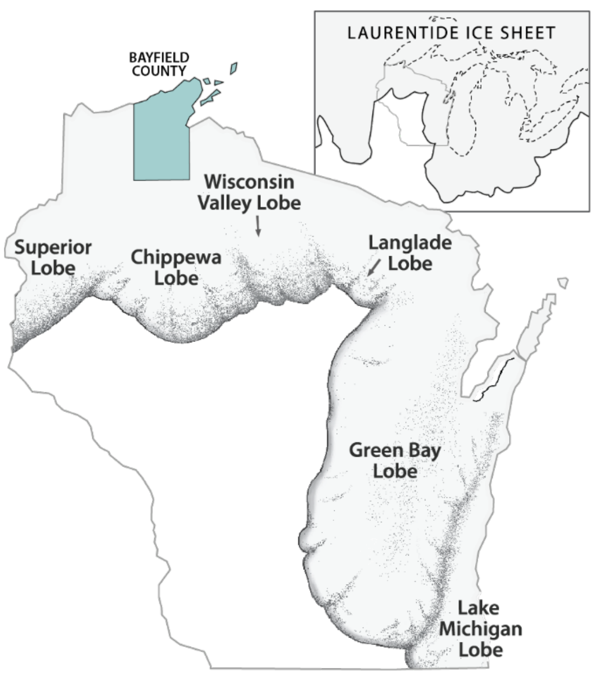

Figure 3. *Map showing the maximum extent of Laurentide Ice Sheet in Wisconsin during the Wisconsin Glaciation; major lobes labeled in black; Bayfield County shaded in green. Inset map shows position of Wisconsin and the Great Lakes within the Laurentide Ice Sheet.*

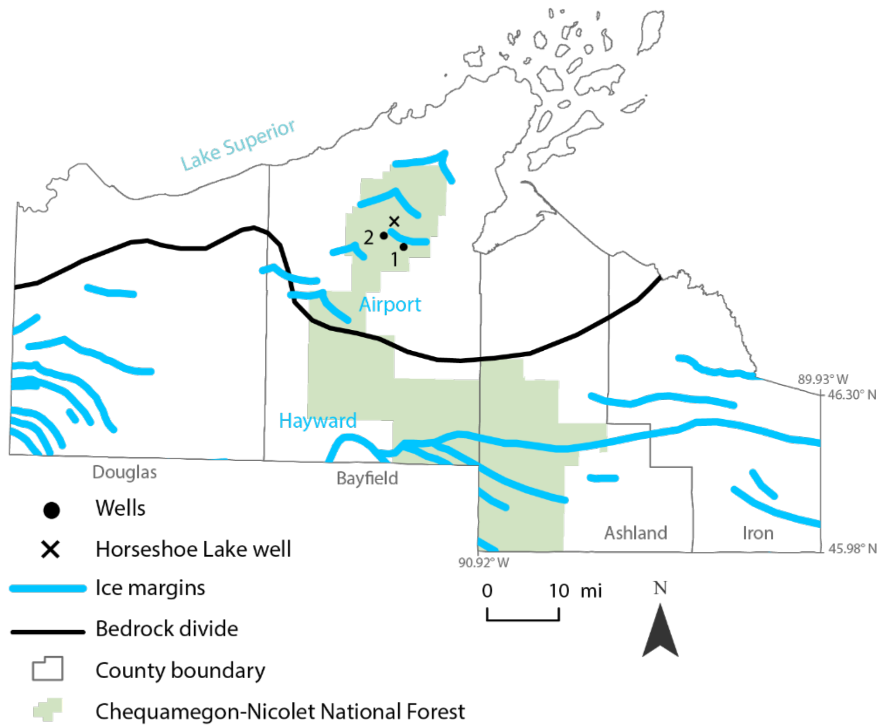

Figure 4. *Map of the study area showing interpreted ice margins and bedrock divide in the Lake Superior region of Wisconsin. Labeled ice margins in Bayfield County (blue text) follow Syverson and others, 2011. County names in gray text.*

In the vicinity of the study area, the sandy uplands are characterized by a thick layer of sandy meltwater stream sediment overlying a thick sequence of sandstone and other sedimentary rock belonging to the Mesoproterozoic Bayfield Group (Nicholson and others, 2006). The corehole locations for this study were mapped as collapsed proglacial stream sediments of the Copper Falls Formation (Clayton, 1984). Little is known about deeper deposits due to a scarcity of subsurface information. Available well logs and passive seismic measurements suggest that the Copper Falls sand is more than 400 ft thick in the study area (Graham and others, 2019). The absolute thickness is uncertain because few nearby geologic logs have encountered bedrock. Well records, mostly situated on the outskirts of the sandy uplands, but including the Horseshoe Lake well (fig. 2), indicate that drilling reached depths of 330–390 ft without encountering bedrock (Graham and others, 2019). Geologic logs in other parts of the sandy uplands reach well over 400 ft without encountering bedrock, including one geologic log about 17 miles southwest of the study area that reported depth to bedrock of 979 ft.

Hydrology and hydrogeology

The sandy uplands of the Bayfield Peninsula are humid and temperate, with an average annual precipitation as recorded from 1981–2010 of approximately 37 inches per year (Thornton and others, 2016). Annual average groundwater recharge ranges from 15 in. to 17 in. (Fehling and others, 2018). Surface drainage is largely absent. Although some lakes are present at the surface, these are perched several hundred feet above the groundwater table (Graham and others, 2019).

The uplands straddle a groundwater divide between Lake Superior to the west and Chequamegon Bay to the east. The absolute water-table elevation in the study area is uncertain because of the lack of groundwater measurements. Published water-table contours were dashed in the sandy uplands to indicate the low level of certainty (Graham and others, 2019).

The Copper Falls Formation sandy meltwater-stream sediment is characterized by relatively high hydraulic conductivity compared to the clayey tills of the Miller Creek Formation and the underlying bedrock of the Bayfield Group (Lenz and others, 2003). Previously simulated values of the Copper Falls sand and gravel hydraulic conductivity range from 30–83 ft/day (Lenz and others, 2003; Leaf and others, 2015; Fehling and others, 2018; Michael Fienen, U.S. Geological Survey, oral commun., 2020). The simulated hydraulic conductivities of the clayey tills of the Miller Creek Formation and the underlying bedrock are typically an order of magnitude lower (Lenz and others, 2003; Leaf and others, 2015).

Methods

Geologic exploration

Rotosonic coring was used to target deep sediments of the Copper Falls Formation at two locations in the Bayfield Peninsula (RS1 and RS2; see fig. 2). The rotosonic coring method is advantageous because it can produce continuous, undisturbed core samples, and can reach hundreds of feet in depth. For this project, rotosonic coring was conducted in 20 ft flights; the core sample diameter was 6 in. and was cased with an 8 in. pipe between flights to minimize resampling of collapsed sediment. Water and drilling mud was circulated during the advancement of the casing but not during sample recovery to avoid sample contamination. Although continuous sample collection is possible, dry, sandy sediments have poorer sample recovery rates than finer sediments. Incomplete sample recovery occurs when friction within the sample barrel exceeds friction outside the barrel, causing the plugged barrel to push through the sediment. Due to incomplete recovery, sample depths are estimates within each 20 ft flight (dataset 1). In addition, boulders can increase the apparent silt content of the sample as they are cut and ground up by the advancing bit (fig. 5d).

Samples from the 20 ft coring flights were divided into 5 ft intervals for temporary storage. Cores were then described, photographed, and representative samples were collected from each 5 ft interval, at lithologic contacts, and within intervals of interest (e.g., fine-grained intervals). Samples are archived at the WGNHS with the high-resolution core photos.

Groundwater wells

Two groundwater wells (MW1 and MW2) were drilled approximately 10–15 ft from the rotosonic cores. The wells were drilled separately from the rotosonic cores because the cores did not appear to reach the water table. The wells were installed with 6 in. steel casing and a 3 ft screen using conventional air rotary water-well drilling methods combined with a casing hammer. Geologic observation was limited to cuttings collected as the drill bit advanced. Because the wells extend deeper than the rotosonic cores, they provided additional but less-detailed geologic data at depth.

A Solinst Barologger was installed in well MW2, and absolute, or unvented, Solinst Leveloggers were installed in both wells. Using the air pressures measured by the Barologger the Levelogger pressures were converted to water levels to obtain a near-continuous record of groundwater elevation in the wells. The transducers were initially set to record every 15 minutes, but this was later adjusted to every 60 minutes due to the consistency of water levels over time. An Onset U30 weather station with a rain gage was installed adjacent to the eastern well (MW1).

Gamma radiation

Down-hole logs of measurements of gamma radiation were collected from the rotosonic core holes and groundwater wells. Gamma logging measures the natural gamma radiation of geologic materials as counts per second (Keys, 1988). Sources for gamma radiation include potassium, uranium, and thorium. Clay and granite often produce higher gamma radiation than sand or carbonate rocks. Gamma radiation can also be elevated somewhat from drilling fluid or boulders that have been ground up by a drill bit (depending on the geochemistry of the boulder).

Water chemistry

Water samples were collected from the wells using a Solinst double-valve pump, and samples from Horseshoe Lake were collected by dipping a sample jar into the water. Electrical conductivity, temperature, and pH were measured in the field using an Oakton PC450 pH/conductivity/temperature meter. Samples were field filtered using a 0.45 µm filter, and analyzed for alkalinity, chloride, nitrogen, and metals at the University of Wisconsin–Stevens Point Water and Environmental Analysis Laboratory (https://www.uwsp.edu/cnr-ap/weal/). Water samples were analyzed for stable isotopes, $\delta^{18}O$ and $\delta^{2}H$, by the Iowa State University Stable Isotope Lab (https://siperg.las.iastate.edu/stable-isotope-lab-sil/).

Results

Two rotosonic cores (RS1 and RS2) and two monitoring wells (MW1 and MW2) were installed in the locations shown on figure 2. Each monitoring well is located approximately 10–15 ft away from the associated abandoned rotosonic core hole. Installation details are shown in tables 1 and 2.

Table 1. Rotosonic boring information.

Rotosonic boring name:	**RS1**	**RS2**
Site identification	Ino-19-01-RS	Ino-19-02-RS
WID[1]	4000360	4000361
Date drilling completed	10/25/2019	10/28/2019
Land surface elevation[2]	1317 ft asl	1242 ft asl
Rotosonic drill depth	280 ft	220 ft
Latitude[3]	46.595062	46.616614
Longitude[3]	–91.154197	–91.212402

[1] WID, or WGNHS ID, is a unique WGNHS identifier for cataloging wells, boreholes, outcrops, and other localities.
[2] Land surface elevation taken from lidar. All elevations reported in feet above mean sea level (ft asl).
[3] Latitude and longitude based on field GPS readings.

Table 2. Monitoring well information.

Monitoring well name:	**MW1**	**MW2**
Site identification	Ino-20-01-MW	Ino-20-02-MW
Adjacent rotosonic boring	Ino-19-01-RS	Ino-19-02-RS
WID[1]	4000362	4000363
WUWN[2]	VQ854	VQ853
Date drilling completed	7/9/2020	7/9/2020
Land surface elevation[3]	1319 ft asl	1245 ft asl
Depth	376 ft	256 ft
Static water depth	305 ft	173 ft
Latitude[4]	46.59502	46.61665
Longitude[4]	–91.15422	–91.21243

[1] WID, or WGNHS ID, is a unique WGNHS identifier for cataloging wells, boreholes, outcrops, and other localities.
[2] WUWN: Wisconsin Unique Well Number.
[3] Land surface elevation taken from lidar. All elevations reported in feet above mean sea level (ft asl).
[4] Latitude and longitude based on field GPS readings.

Stratigraphy

The eastern rotosonic boring (RS1) was 280 feet deep, with approximately 75% sample recovery (figs. 5 and 6; dataset 1). In general, core sections with sandy sediment typically had poor recovery. The majority of the sediment collected in the eastern core was well-sorted sand, or sand and gravel that is interpreted to be meltwater stream sediment. Cobbles and boulders

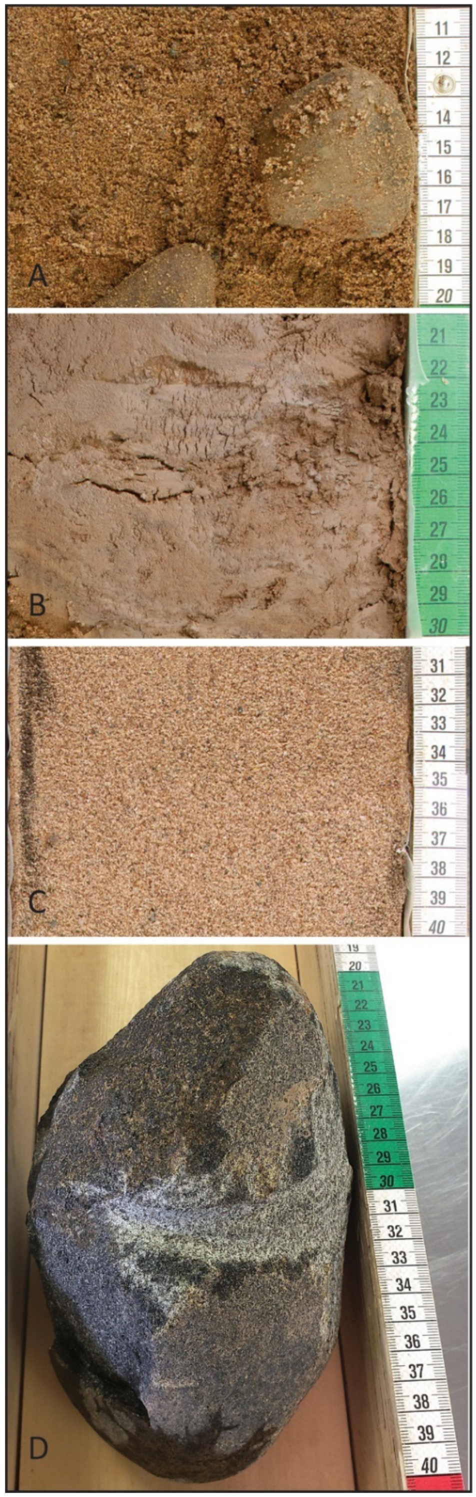

Figure 5. *Photos of typical sediment types in core RS1 with interpreted depositional environment for these sediment types: (panel A) sand and gravel (stream sediment), (panel B) laminated silty clay (lake sediment), (panel C) sand (stream sediment), and (panel D) rock ground by the core bit, which may create gray dust in samples. Measuring tape in cm for scale.*

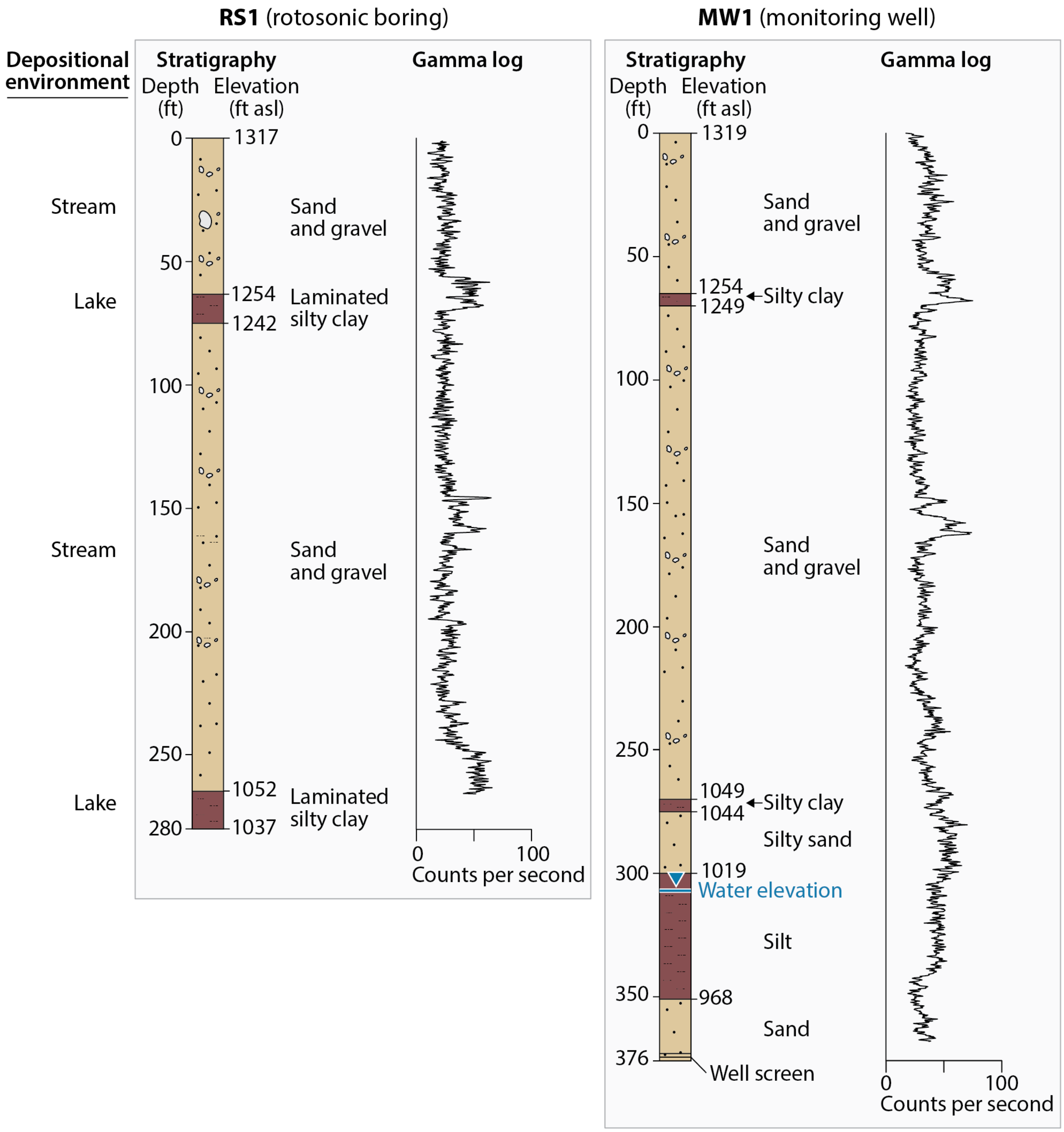

Figure 6. *Stratigraphic column and gamma log measurements for rotosonic boring RS1 and monitoring well MW1 with interpreted depositional environments. The stratigraphic column for MW1 has less detail than RS1 because of the less detailed sampling method. Water elevation based on average WGNHS measurements. Note that surface elevations differ so depths are not equivalent.*

were commonly observed (fig. 5a and d). Two finer-grained, laminated intervals were observed at 63–75 ft depth and 265–280 ft depth (1254–1242 feet above mean sea level (ft asl) and 1052–1037 ft asl) that are interpreted to be lake sediment (fig. 5b). Sediment was dry throughout the core.

The adjacent monitoring well (MW1) to RS1 extended nearly 100 ft deeper than the rotosonic boring (fig. 6). Cuttings from MW1 generally correlated with those from the adjacent RS1 in overlapping depth zones. Below 280 ft (the bottom depth of RS1), sediment observed in the cuttings included a thick layer of silt from approximately 300–350 ft deep, overlying a fine sand. This silt layer supports the interpretation that the sediment from this interval was deposited in a lake. Water elevation was observed at a depth of 305 ft, and the well screen was set at 376 ft within the sand below the silty layer.

The observed gamma radiation is elevated in both cores at the same depth as fine-grained intervals (fig. 6). However, in some places the gamma response is offset by a few feet from the observed intervals of fine-grained sediment, such as from 1254–1242 ft asl in RS1. Gamma radiation is also elevated for longer intervals than the observed occurrence of fine-grained materials in MW1 from 1254–1249 ft asl and 1049–968 ft asl. These differences in depth between the observed core materials and the gamma responses may be a result of the poor recovery in some sections of the RS1 core, the inherent imprecision of depth measurements during drilling, and the mixing of materials that can occur during cutting recovery. Furthermore, both gamma logs detected higher gamma counts at approximately 150 ft depth in a sand and gravel unit. The cause of the higher gamma radiation is unknown. Possible causes include unrecovered fine-grained sediment, a change in the source rock for the sand and gravel (e.g., gravel with high feldspar content), or nearby boulders. This section of the core had only approximately 50% recovery (dataset 1), and thin, broken, fine-grained sediment was recorded between 160–165 feet. It is likely that the increase in gamma radiation at about 150 ft depth reflects a thin, fine-grained interval not recovered in the core.

The western rotosonic boring (RS2) was 220 feet deep, with around 80% sample recovery (figs. 7 and 8). Similar to RS1, the majority of sediment collected in the core was sand and gravel or well-sorted sand that is interpreted to have been deposited by meltwater streams. Cobbles and boulders were present, but less commonly observed than for RS1 (fig. 7a). Finer-grained laminated sediment interpreted as lake sediment was observed at a depth of 109–115 ft (1133–1127 ft asl; fig. 7b). Three sandy diamicts that are interpreted as till deposited by the Superior Lobe (fig. 7c) were observed at depths of 115–122 ft, 143–153.5 ft, and 199–203 ft (1127–1120 ft asl, 1099–1089 ft asl, and 1043–1039 ft asl).

Monitoring well MW2 reached 256 ft deep, extending about 30 ft deeper than RS2. Most of the stratigraphy is similar to RS2, except that fine-grained intervals found in RS2 at about 115 ft and 200 ft depth were not observed in the well cuttings. However, logs from MW2 and RS2 indicate that recorded gamma radiation is elevated in both logs at these intervals (fig. 8). Because the fine-grained intervals found in RS2 were relatively thin, it is likely that the layers are present in MW2, but simply were not collected in the cuttings. As in RS1, the gamma response is offset by a few feet from the observed fine-grained intervals in RS2. This is likely due to problems with recovery of the dry, sandy material throughout the core, and associated challenges in estimating depths. Static water was measured at a depth of 173 ft in MW2.

Although the two borings are only about 3.2 miles apart, there is little correlation between fine-grained units (fig 9). This sediment heterogeneity is evident on the land surface as well. Even though the uplands are dominantly sand, surface water is perched in lakes hundreds of feet above the water table, suggesting that there are local deposits of fine-grained sediments.

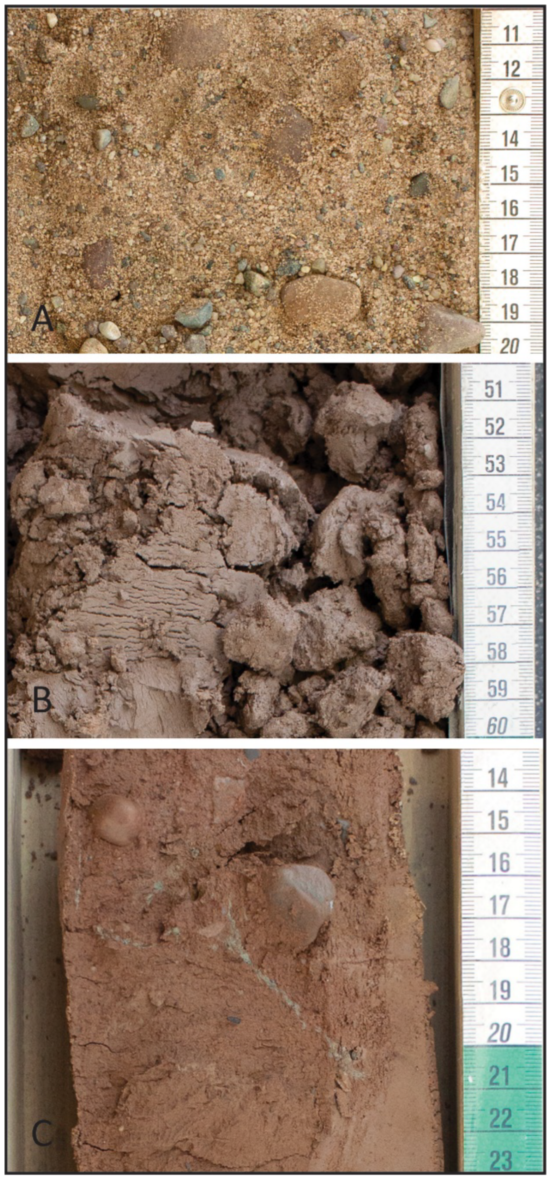

Figure 7. *Photos of typical sediment types in core RS2 and interpreted depositional environment for these sediment types: (panel A) sand and gravel (stream sediment), (panel B) laminated silty clay (lake sediment), and (panel C) sandy diamict (till). Measuring tape in cm for scale.*

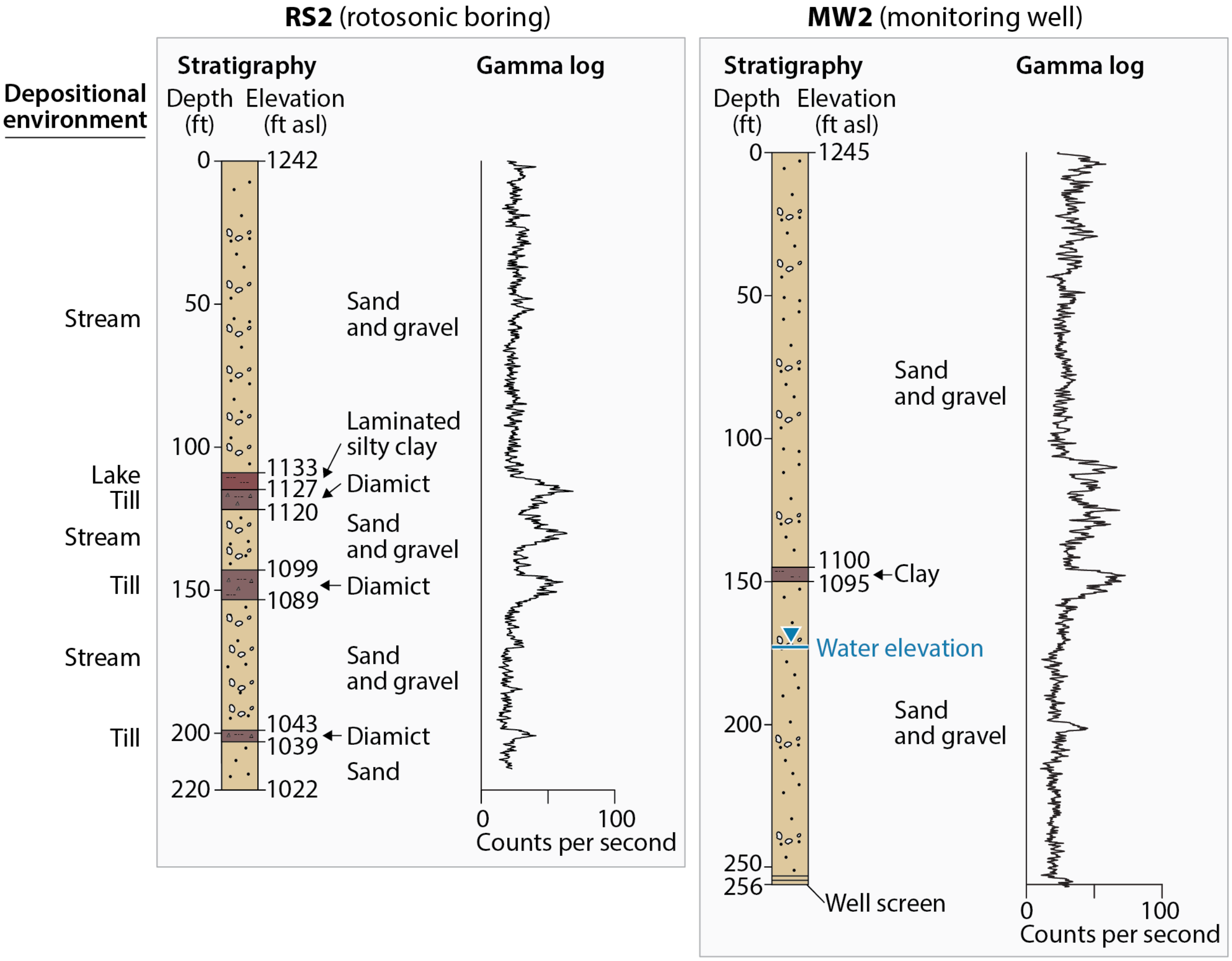

Figure 8. *Stratigraphic column and gamma log measurements for rotosonic boring RS2 and monitoring well MW2 with interpreted depositional environments. The stratigraphic column for MW2 has less detail than RS2 because of the less detailed sampling method. Water elevation based on average WGNHS measurements. Note that surface elevations differ so depths are not equivalent.*

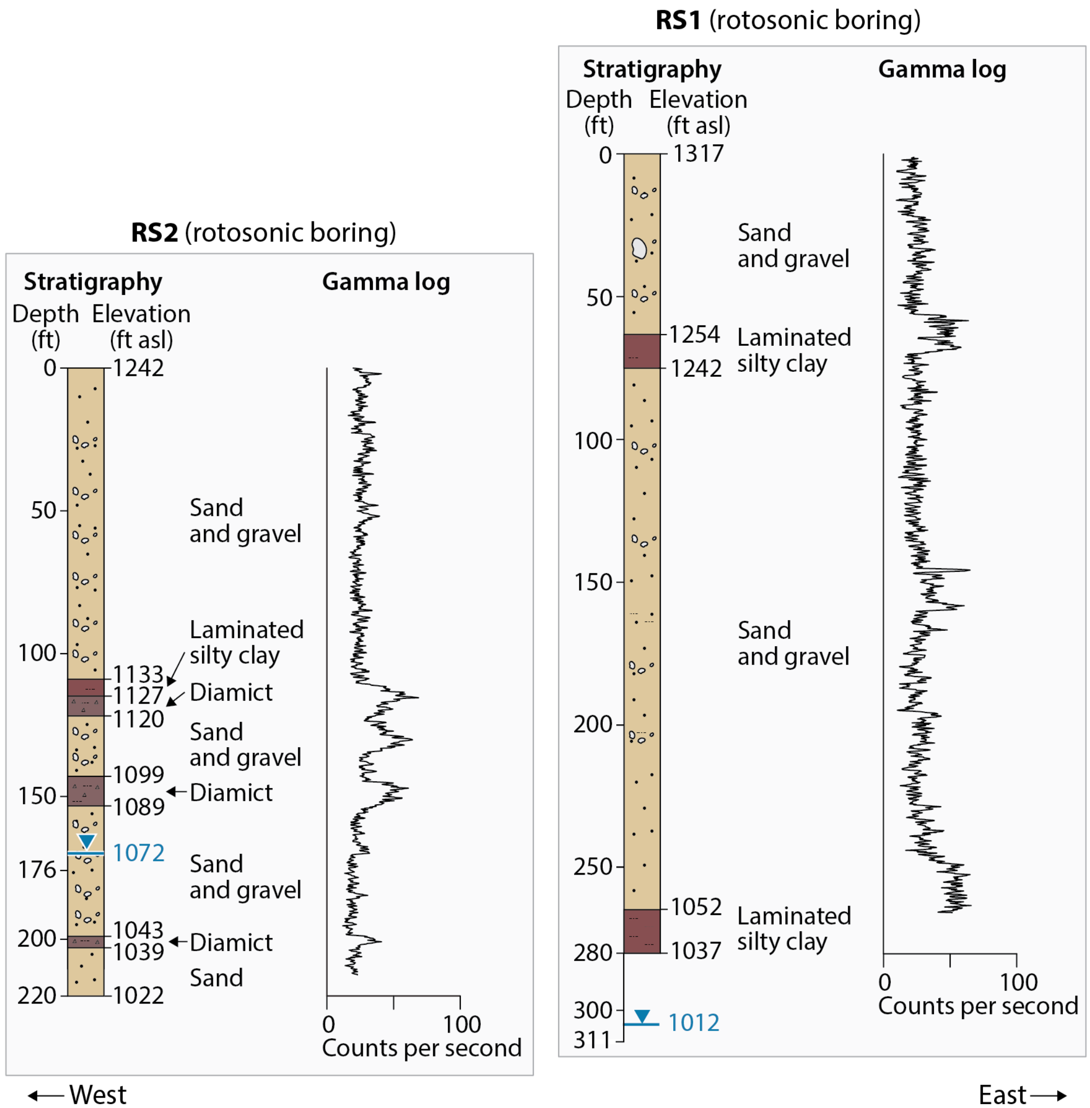

Figure 9*. Stratigraphic columns for rotosonic borings RS1 and RS2 aligned by elevation. Water elevations, denoted by blue triangles, are based on average WGNHS measurements. Note that the surface elevations differ so depths are not equivalent.*

Groundwater levels

The pressures measured by the Solinst Leveloggers in wells MW1 and MW2 are affected both by changes in barometric pressure and actual water-level variations (fig. 10). For shallow water tables, the downward propagation of air pressure through pore spaces is so fast that the pressure difference between the well and the aquifer is negligible. In this situation, unvented pressure transducer readings are compensated for by using corresponding barometric pressure measurements. For deep water tables, as in the Bayfield Peninsula, downward propagation of air pressure through pores of the unsaturated zone can be delayed. This results in an imbalance in atmospheric pressure within the well-aquifer system, and an inverse relationship between water level and barometric pressure measurements (Weeks, 1979; Spane, 2002; Butler and others, 2011). Figure 11 shows the water-level data series after removing the effects of barometric pressure changes using the Kansas Geological Survey barometric response function software (Bohling and others, 2011).

The WGNHS rain gage near MW1 records precipitation, which is included in Figure 11. However, this rain gage is not heated during the winter months, so water equivalent of snowfall is not directly measured at the site. Instead, water equivalent of snowfall was calculated using a typical snow-to-liquid ratio of 10:1 and snowfall records from the Global Historical Climatology Network (GHCN) US1WIBY0014 station, which is located about 3.6 miles to the east of the study site (NCEI, 2022). The rainfall record for the GHCN:US1WIBY0014 station was also used between April 25, 2022, and June 30, 2022, because a rainfall record for the rain gage near MW1 was unavailable.

Water levels at MW1 ranged from 1011.31 ft asl to 1013.47 ft asl between July 2020 and June 2022, and water levels at MW2 ranged from 1071.28 ft asl to 1072.68 ft asl over the same time period (fig. 11). Water levels for the Horseshoe Lake well, located 2.3 miles to the northeast of MW2 (fig. 2), are considered approximate. The water level measurements using the air line may only be accurate to 1 foot or more (Cunningham and Schalk, 2011). They are, however, lower than those at MW2 and higher than those at MW1 (fig. 11).

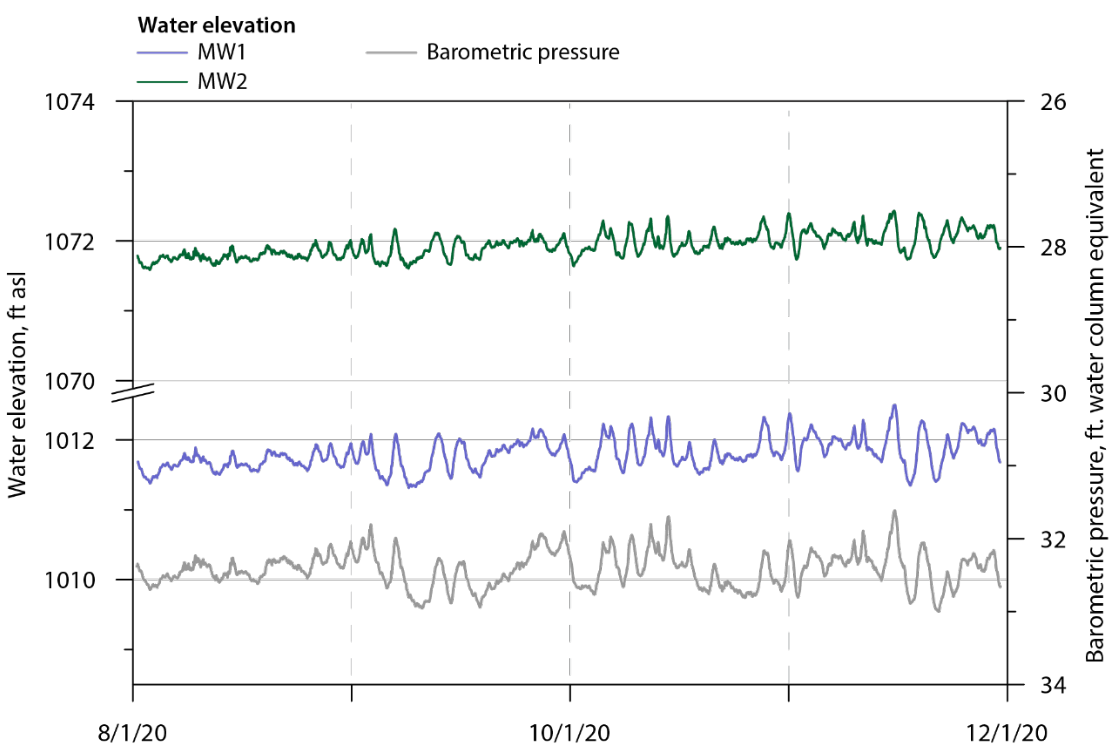

Figure 10. *Measurements of uncorrected water elevations and barometric pressure from August 2020 to December 2020. Barometric pressure measured from transducer hung in the airspace in MW1.*

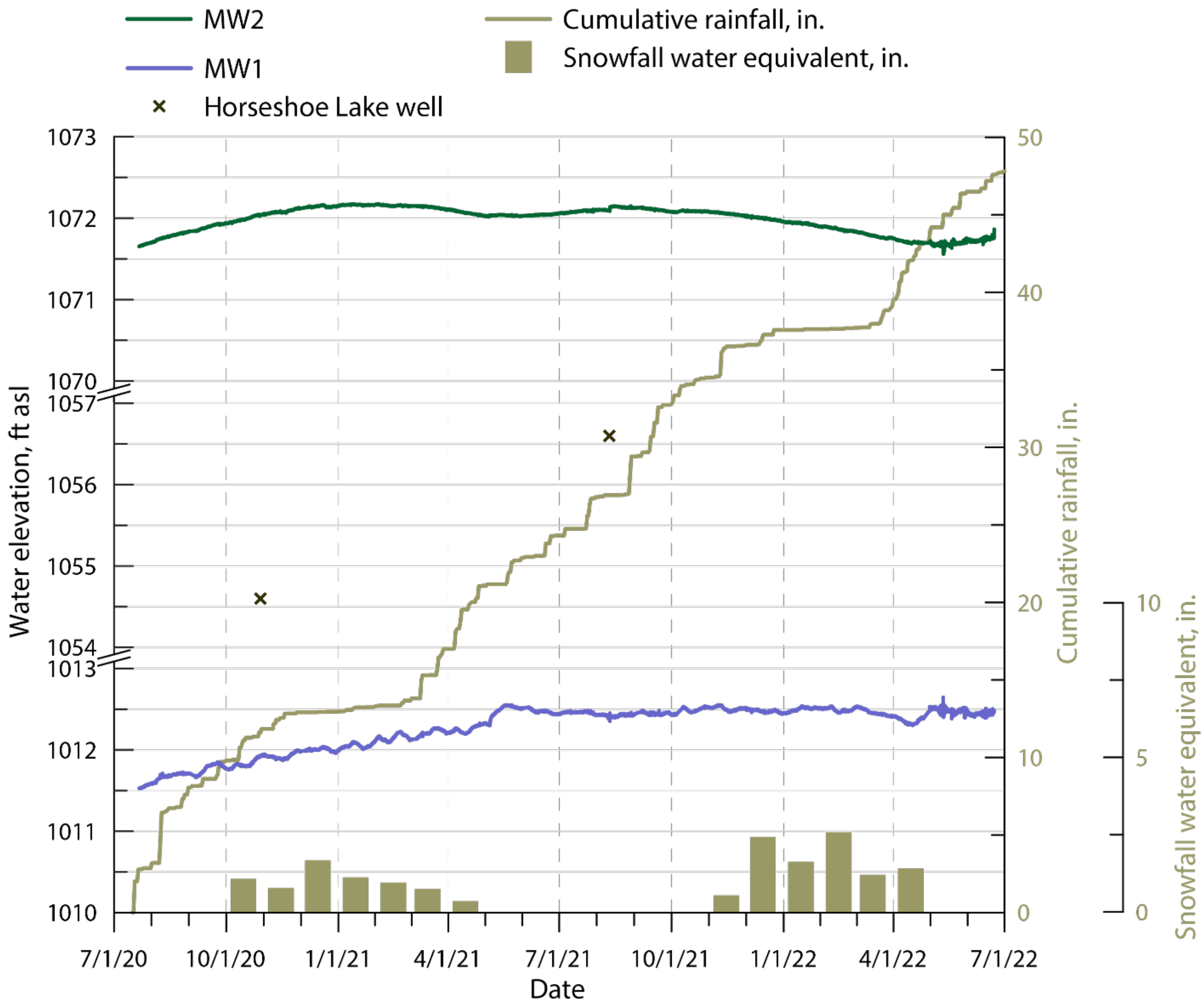

Figure 11. *Graph showing corrected water elevations, cumulative rainfall from the WGNHS rain gage (July 2020–April 2022) and the GHCN:US1WIBY0014 station (late April 2022–June 2022), and snowfall water equivalent from the GHCN:US1WIBY0014 station.*

Water levels at MW2 rose by approximately 0.5 ft from the beginning of the record in July 2020 to January 2021 (fig. 11; dataset 2). Water levels fell between January 2021 and May 2021. This seasonal pattern in the record continued, but water levels rose over a shorter duration (May 2021 to August 2021) and to a lesser extent. Between August 2021 and May 2022, water levels at MW2 fell approximately 0.5 ft. In May 2022, water levels began to rise again. A seasonal pattern is less apparent in the MW1 record. Water levels at MW1 rose approximately 1 ft from July 2020 to June 2021, then remained mostly stable until the end of the record in June 2022.

Chemistry

MW1, MW2, the Horseshoe Lake well, and Horseshoe Lake have very low total dissolved solids (TDS) concentrations based on 3 to 4 samples from each location (table 3, dataset 3). The three wells have fairly similar water quality, as depicted on Stiff plots in figure 12. Stiff plots, which include cation and anion concentrations in milliequivalents per liter (meq/L), allow for a visual comparison of TDS concentrations among different sampling locations. The three wells have an average TDS concentration of 58 mg/L. Horseshoe Lake has the lowest TDS (10 mg/L), which suggests that direct precipitation and snowmelt are the dominant water sources to the lake. Similarly, the average specific conductance in MW1, MW2, and the Horseshoe Lake well is lower (88 µS/cm at 25°C) than the average for wells elsewhere in the Washburn-Great Divide Unit of the Chequamegon-Nicolet National Forest (183 µS/cm at 25°C; Fehling and others, 2018), suggesting that groundwater residence times (time in contact with aquifer materials) are relatively short, or that aquifer materials have low clay or carbonate content. This is consistent with our understanding of the study area as a recharge zone, and the sandy, silicate-rich materials collected in the rotosonic borings.

Table 3. Dates of sampling at each sample location.

Sampling location	Sept. 2012[1]	May 2021	Aug. 2021	Oct. 2021	Apr. 2022
MW1		X	X	X	X
MW2		X	X	X	X
Horseshoe Lake well	X		X	X	
Horseshoe Lake	X		X	X	

[1] From Fehling and others (2018).

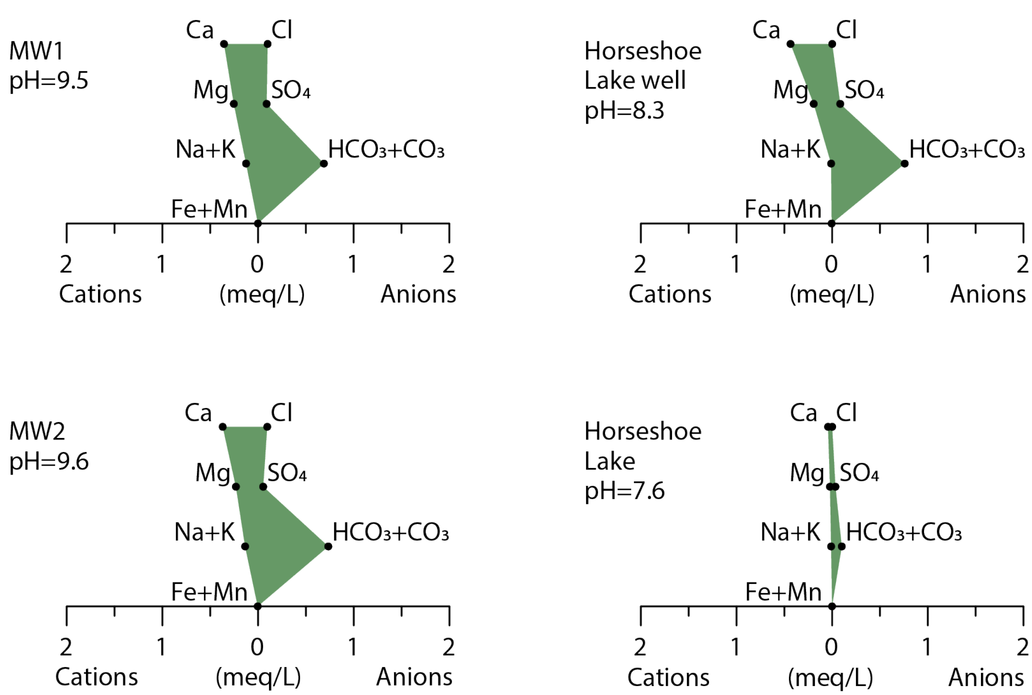

Figure 12. *Stiff plots of average major ion constituents in milliequivalents per liter (meq/L), showing that the three wells sampled for this study (MW1, MW2, Horseshoe Lake Well) have similar total dissolved solids (TDS) concentrations, and Horseshoe Lake has a different TDS concentration.*

The water samples collected from the three wells and Horseshoe Lake (table 3) were also analyzed for stable isotopes of oxygen and hydrogen, which are measured as a ratio of the two most abundant isotopes of each element (^{18}O and ^{16}O or ^{2}H and ^{1}H, respectively). Isotopic concentrations are expressed as the difference between the measured ratios of the sample and a standard over the measured ratio of the standard, and are reported as parts per thousand using delta (δ) notation. A plot of $\delta^{2}H$ versus $\delta^{18}O$, as in figure 13, can be used to provide information on sources of groundwater and surface water, or to investigate secondary processes such as evaporation. A local meteoric water line (LMWL) that represents the isotopic variation in precipitation for a region is often included on the plot. Partitioning of groundwater

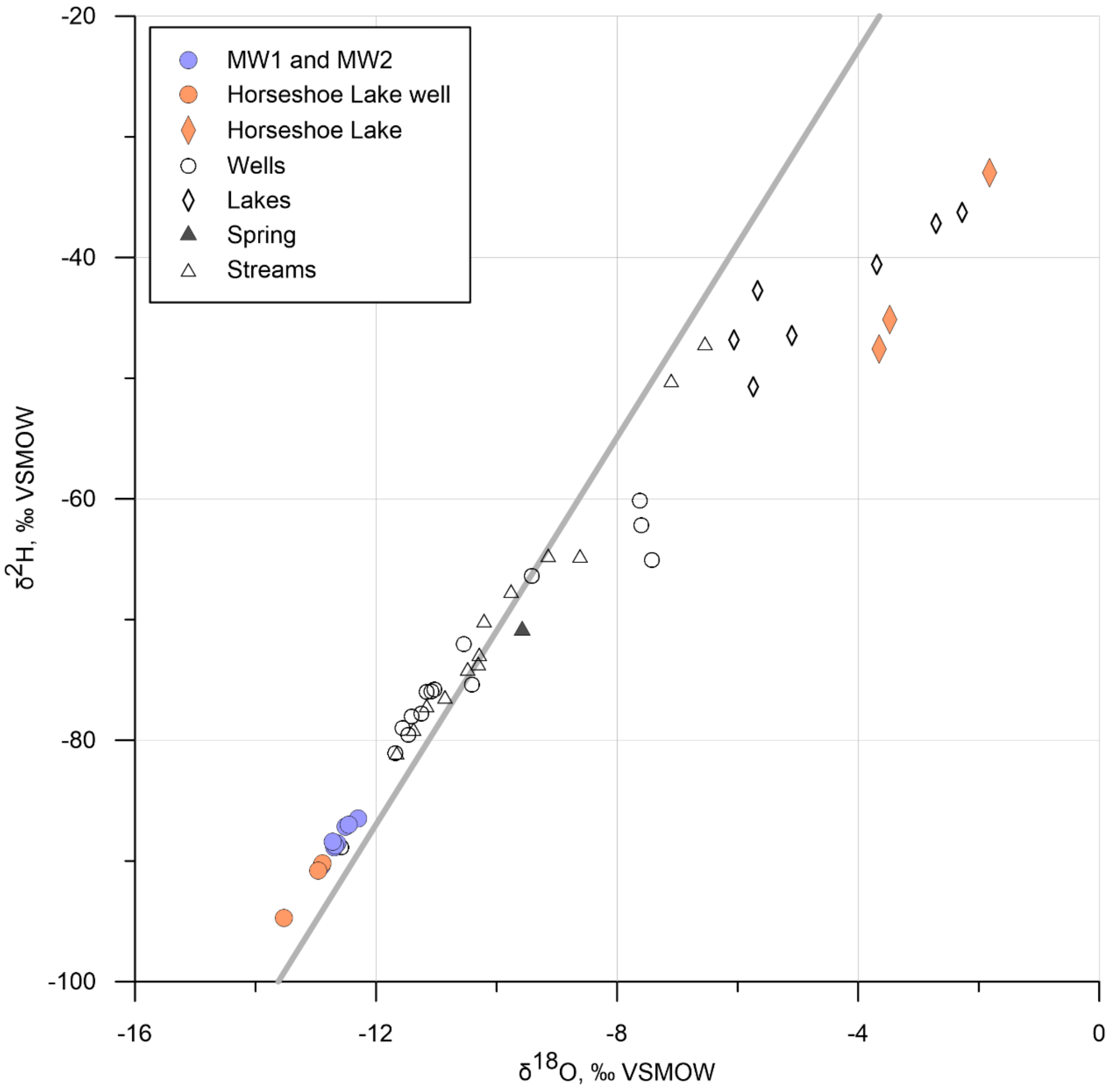

Figure 13. *Plot of stable isotope analysis results for the MW1, MW2, and Horseshoe Lake wells, Horseshoe Lake, and other water samples from the Washburn-Great Divide Unit of the Chequamegon-Nicolet National Forest (Fehling and others, 2018), with the local meteoric water line (Krabbenhoft and others, 1990) plotted in gray. MW: monitoring well; ‰ = parts per thousand; VSMOW: the stable isotope standard Vienna Standard Mean Ocean Water.*

and surface-water samples along the LMWL can provide information on groundwater recharge environments and seasonality. Samples that plot to the right of the LMWL are indicative of processes that fractionate oxygen and hydrogen isotopes, such as evaporation (Clark and Fritz, 1997).

The stable isotope ratios measured in the MW1, MW2, and Horseshoe Lake wells are some of the lowest values measured in the Washburn-Great Divide Unit of the Chequamegon-Nicolet National Forest (Fehling and others, 2018), plotting to the lower left of the graph in figure 13. This is indicative of cold source water, likely snowmelt recharge. Similar to other lakes in the region, the stable isotope measurements for Horseshoe Lake plot to the right of the LMWL, indicating evaporative effects.

Discussion

Aquifer characteristics

Materials observed in cores and cuttings were mostly sand and gravel or well-sorted sand that were likely deposited by meltwater streams. However, coarser sediment (cobbles and boulders) were common, and finer-grained laminated intervals were also observed. The lack of correlation between cores as well as the presence of perched lakes in the area suggests that the subsurface of the Bayfield Peninsula is heterogeneous. Although the region lacks an extensive regional aquitard, the presence of fine-grained sediments likely affects groundwater movement locally.

Water levels

The two new wells and the Horseshoe Lake well are screened below the water table; therefore, the water elevations cannot be considered equal to the water table unless there is zero vertical gradient. Water quality results are consistent with our understanding of the study area as a recharge zone. Fine-grained layers are present at depth, and locally perched lakes are present in the region. These conditions all suggest the likelihood of non-zero downward vertical gradients. Water levels in wells MW1 and MW2 and the Horseshoe Lake well are also lower than the mapped water table (Graham and others, 2019) generated from a regional groundwater flow model (Fehling and others, 2018; Leaf and others, 2019). If the Bayfield County water-table map is correct, this would indicate a downward hydraulic gradient of approximately 0.3 ft/ft to 0.5 ft/ft. The actual water table, while still uncertain, is likely between the measured water levels and the simulated water-table map.

There appears to be a lag of approximately two months between spring snowmelt and/or spring rainfall and groundwater recharge at MW2, yet a similar pattern does not exist at MW1. Notably, the fine-grained interval from 300–350 ft deep at MW1 may be creating semi-confined conditions at this well location. Because the water levels in the wells follow different patterns, and neither respond rapidly to precipitation, this suggests that there is significant redistribution of water in the unsaturated zone. The timing and distribution of groundwater recharge in the sandy uplands may be different from what would be expected in an area with a shallower water table. These findings also have implications for contaminant transport in the sandy uplands, and they underscore the need to better understand water movement in both the unsaturated and the saturated zones.

Summary

Data from two new cores and wells, one existing well, and a lake in the sandy uplands of the Bayfield Peninsula provide information about the local hydrogeology and contribute to the understanding of the regional groundwater system. Future well water levels will be reported with data from the Wisconsin Groundwater-Level Monitoring Network (https://wgnhs.wisc.edu/water-environment/groundwater-monitoring-network/).

Supplemental material

Supplemental material in this report includes rotosonic core data, water level measurements, and water chemistry measurements. See the WGNHS Publication Catalog to download these data: https://doi.org/10.54915/znsx3519.

Dataset 1: Rotosonic core data from the sandy uplands of the Bayfield Peninsula, Wisconsin
Two spreadsheets (.csv) with rotosonic core descriptions and percent recovery.

Dataset 2: Water-level measurements from two monitoring wells in the sandy uplands of the Bayfield Peninsula, Wisconsin
Two spreadsheets (.csv) with measured water elevations in wells MW1 and MW2. The water levels are reported prior to correction for the effects of barometric pressure changes.

Dataset 3: Water chemistry field measurements, major ion sampling results, and stable isotope sampling results from three wells and a lake in the sandy uplands of the Bayfield Peninsula, Wisconsin
Three spreadsheets (.csv) with water chemistry sampling results. The spreadsheets include results from laboratory analysis from the University of Wisconsin–Stevens Point Water and Environmental Analysis Laboratory, field measurements, and stable isotope analyses.

Acknowledgments

We thank Tom Fitz (Northland College), Greg Knight (USFS), Kacie Stolzman (WGNHS), and Dave Ullman (Northland College), who provided valuable input and support that improved the quality of this report. This work was supported by USFS Agreement No. 15-GN-11091300-1096.

References

Bohling, G.C., Jin, W., Butler, J.J., Jr., 2011, Kansas Geological Survey barometric response function software user's guide: Kansas Geological Survey Open File Report 2011-10, 23 p., https://www.kgs.ku.edu/HighPlains/OHP/index_program/KGS_BRF_Manual.pdf.

Bradbury, K.R., Leaf, A.T., Hunt, R.J., Juckem, P.F., Fehling, A.C., Mauel, S.W., and Schoephoester, P.R., 2018, Characterization of groundwater resources in the Chequamegon-Nicolet National Forest, Wisconsin: Medford Unit: Wisconsin Geological and Natural History Survey Technical Report 004-1, 50 p., 10 pl., https://wgnhs.wisc.edu/catalog/publication/000961/resource/tr0041.

Breckenridge, A., 2013, An analysis of the late glacial lake levels within the western Lake Superior basin based on digital elevation models: Quaternary Research, v. 80, no. 3, p. 383–395, https://doi.org/10.1016/j.yqres.2013.09.001.

Butler, J.J., Jr., Jin, W., Mohammed, G.A., and Reboulet, E.C., 2011, New insights from well responses to fluctuations in barometric pressure: Groundwater, v. 49, no. 4, p. 525–533, https://doi.org/10.1111/j.1745-6584.2010.00768.x.

Clark, I.D., and Fritz, P., 1997, Environmental Isotopes in Hydrogeology, Boca Raton, FL: CRC Press, 342 p., https://doi.org/10.1201/9781482242911.

Clayton, L., 1984, Pleistocene geology of the Superior Region, Wisconsin: Wisconsin Geological and Natural History Survey Information Circular 46, 40 p., 1 pl., scale 1:250,000, https://wgnhs.wisc.edu/pubs/000296/.

Cunningham, W.L., and Schalk, C.W., comps., 2011, GWPD13—Measuring water levels by use of an air line: Groundwater Technical Procedures of the U.S. Geological Survey GWPD13, *in* U.S. Geological Survey Techniques and Methods 1–A1, p. 111–116, https://pubs.usgs.gov/tm/1a1.

Fehling, A.C., Bradbury, K.R., Leaf, A.T., Pruitt, A., Hunt, R.J., Mauel, S.M., Schoephoester, P.R., and Juckem, P.F., 2018, Characterization of groundwater resources in the Chequamegon-Nicolet National Forest, Wisconsin: Washburn/Great Divide Unit: Wisconsin Geological and Natural History Survey Technical Report 004-4, 60 p., https://wgnhs.wisc.edu/pubs/tr0044/.

Fehling, A.C., and Hart, D.J., 2021, Potential effects of climate change on stream temperature in the Marengo River headwaters: Wisconsin Geological and Natural History Survey Bulletin 115, 74 p., 3 pl., 3 datasets, https://wgnhs.wisc.edu/pubs/000976.

Fitzpatrick, F.A., Peppler, M.C., Saad, D.A., Pratt, D.M., and Lenz, B.N., 2015, Geomorphic, flood, and groundwater-flow characteristics of Bayfield Peninsula streams, Wisconsin, and implications for brook-trout habitat: U.S. Geological Survey Scientific Investigations Report 2014-5007, 80 p., http://dx.doi.org/10.3133/sir20145007.

Graham, G.E., Fehling, A.C., Gotkowitz, M.B., and Bradbury, K.R., 2019, Hydrogeologic atlas of Bayfield County, Wisconsin: Wisconsin Geological and Natural History Survey Technical Report 005, 25 p., 5 plates, scale 1:100,000, https://wgnhs.wisc.edu/catalog/publication/000967.

Keys, W.S., 1988, Borehole geophysics applied to ground-water investigations: U.S. Geological Survey Open-File Report 87-539, 305 p., https://doi.org/10.3133/ofr87539.

Krabbenhoft, D.P., Bowser, C.J., Anderson, M.P., Valley, J.W., 1990, Estimating groundwater exchange with lakes: 1. The stable isotope mass balance method: Water Resources Research, v. 26, no. 10, p. 2445–2453, https://doi.org/10.1029/WR026i010p02445.

Leaf, A.T., Fehling, A., Bradbury, K.R., Hunt, R.J., and Juckem, P.F., 2019, GFLOW model used to characterize the groundwater resources of the Great Divide Unit of the Chequamegon-Nicolet National Forest, Wisconsin: U.S. Geological Survey Water Mission Area NSDI Node, https://doi.org/10.5066/F708648W.

Leaf, A.T., Fienen, M.N., Hunt, R.J., and Buchwald, C.A., 2015, Groundwater/surface-water interactions in the Bad River Watershed, Wisconsin: U.S. Geological Survey Scientific Investigations Report 2015-5162, 110 p., http://dx.doi.org/10.3133/sir20155162.

Lenz, B.N., Saad, D.S., and Fitzpatrick, F.A., 2003, Simulation of ground-water flow and rainfall runoff with emphasis on the effects of land cover, Whittlesey Creek, Bayfield County, Wisconsin, 1999–2001: U.S. Geological Survey Water-Resources Investigations Report 20003-4130, 47 p., https://doi.org/10.3133/wri034130.

National Centers for Environmental Information (NCEI), 2022, Climate Data Online (CDO), database accessed May 20, 2022 and July 11, 2022, at https://www.ncdc.noaa.gov/cdo-web/.

Nicholson, S.W., Cannon, W.F., Woodruff, L.G., and Dicken, C.L., 2006, Bedrock geologic map of the Port Wing, Solon Springs, and parts of the Duluth Sandstone 30’ × 60’ quadrangles, Wisconsin and Minnesota: U.S. Geological Survey Scientific Investigations Map 2869, scale 1:100,000, https://doi.org/10.3133/sim2869.

Spane, F.A., 2002, Considering barometric pressure in groundwater flow investigations: Water Resources Research, v. 38, no., 6, p. 14-1 – 14-18, https://doi.org/10.1029/2001WR000701.

Syverson, K.M., Clayton, Lee, Attig, J.W., and Mickelson, D.M., eds., 2011, Lexicon of Pleistocene Stratigraphic Units of Wisconsin: Wisconsin Geological and Natural History Survey Technical Report 1, 180 p., https://wgnhs.wisc.edu/catalog/publication/000555.

Thornton, P.E., Thornton, M.M., Mayer, B.W., Wei, Y., Devarakonda, R., Vose, R.S., and Cook, R.B., 2016, Daymet: Daily Surface Weather Data on a 1-km Grid for North America, version 3: Oak Ridge National Laboratory Distributed Active Archive Center, http://dx.doi.org/10.3334/ORNLDAAC/1328.

Weeks, E.P., 1979, Barometric fluctuations in wells tapping deep unconfined aquifers: Water Resources Research, v. 15, no. 5, p. 1167–1176, https://doi.org/10.1029/WR015i005p01167.